JPET Fast Forward. Published on July 14, 2020 as DOI: 10.1124/jpet.120.265835
This article has not been copyedited and formatted. The final version may differ from this version.

JPET # 265835

Dextromethorphan and dextrorphan influence insulin secretion by interacting with K_{ATP} and L-type Ca^{2+} channels in pancreatic β-cells

Anne Gresch, Martina Düfer

University of Münster, Pharmaceutical and Medicinal Chemistry, Dept. of Pharmacology, Corrensstraße 48, 48149 Münster, Germany

JPET # 265835

Running Title: NMDA receptor antagonists and β-cells

Section assignment for table of contents: Endocrine and Diabetes

Address correspondence to:

Prof. Dr. Martina Düfer

Pharmaceutical and Medicinal Chemistry, Dept. of Pharmacology

PharmaCampus

Corrensstraße 48, 48149 Münster, Germany

Phone: +49 251 83 33339; Fax: +49 251 83 32144

martina.duefer@uni-muenster.de

Text pages: 18

Tables: 0

Figures: 6

References: 42

Word count:

Abstract: 250

Introduction: 614

Discussion: 1712

Key words: β-cell, cytosolic calcium, dextromethorphan, insulin secretion, NMDA receptor, K_{ATP} channel

Abbreviations: a.u.: arbitrary fluorescence units, DXM: dextromethorphan, DXO: dextrorphan, FOPP: fraction of plateau phase, MEA: microelectrode array, NMDA: N-methyl-D-aspartate, SUR1-KO: sulfonylurea receptor 1 knockout

Abstract

The NMDA receptor antagonist dextromethorphan (DXM) and its metabolite dextrorphan (DXO) have been recommended for treatment of type 2 diabetes mellitus because of beneficial effects on insulin secretion. This study investigates how different key points of the stimulus-secretion coupling in mouse islets and β-cells are influenced by DXM or DXO. Both compounds elevated insulin secretion, electrical activity and $[Ca^{2+}]_c$ in islets at a concentration of 100 µM along with a stimulating glucose concentration. DXO and DXM increased insulin secretion approximately 30-fold at a substimulatory glucose concentration (3 mM). Patch-clamp experiments revealed that 100 µM DXM directly inhibited K_{ATP} channels by about 70 %. Of note, DXM decreased the current through L-type Ca^{2+} channels about 25 %, leading to a transient reduction in Ca^{2+} action potentials. This interaction might explain why elevating DXM to 500 µM drastically decreased insulin release. DXO inhibited K_{ATP} channels almost equally. In islets of K_{ATP} channel-deficient SUR1 knockout mice the elevating effects of 100 µM DXM on $[Ca^{2+}]_c$ and insulin release were completely lost. By contrast, 100 µM DXO still increased glucose-stimulated insulin release around 60 %. In summary, DXM-induced alterations in stimulus-secretion coupling of wildtype islets result from a direct block of K_{ATP} channels and are partly counteracted by inhibition of L-type Ca^{2+} channels. The stimulatory effect of DXO seems to be based on a combined antagonism on K_{ATP} channels and NMDA receptors and already occurs under resting conditions. Consequently, both compounds seem not to be suitable candidates for treatment of type 2 diabetes mellitus.

Significance Statement

This study shows that the use of dextromethorphan as an antidiabetic drug can cause unpredictable alterations in insulin secretion by direct interaction with K_{ATP} and L-type Ca^{2+} channels besides its actual target, the NMDA receptor.

Introduction

Dextromethorphan (DXM) is known as a non-opioid, over-the-counter cough suppressant. Currently, there are many clinical studies investigating the therapeutic potential of DXM mainly for treatment of diseases related to the central nervous system. Suggested indications are depression, traumatic brain injury, stroke, seizure, pain, methotrexate neurotoxicity, Parkinson's disease and autism (Nguyen et al., 2016). In 2010, the FDA approved the use of DXM in combination with quinidine for patients suffering from pseudobulbar affect. Apart from its neuroprotective properties, DXM has been suggested for treatment of type 2 diabetes mellitus (Marquard et al., 2015; Marquard et al., 2016). These versatile effects are based on the antagonism of DXM at the NMDA receptor (NMDAR). The NMDAR is a voltage- and ligand-gated ion channel that opens selectively for cations (especially Na^+, K^+ and Ca^{2+}) upon activation. The heterotetrameric channel is activated by concurrent depolarization to release the Mg^{2+} block out of the pore and by simultaneous binding of its ligand and a co-activator (e. g. glycine) (Vyklicky et al., 2014; Zhu et al., 2016). In the nineties it became evident that NMDARs exist in insulin-secreting β-cells and take part in the regulation of glucose-induced insulin secretion (Gonoi et al., 1994; Inagaki et al., 1995; Molnar et al., 1995). There are controversial results about the function of NMDARs. Inhibition of the NMDAR either results in increased insulin secretion (Marquard et al., 2015), in no alteration of insulin secretion (Bertrand et al., 1992; Chan et al., 1997; Patterson et al., 2016; Imai et al., 2018; Suwandhi et al., 2018) or in reduced insulin secretion (Patterson et al., 2016). The exact molecular mechanism is not clear yet but it was demonstrated that NMDAR activity contributes to the trafficking of K_{ATP} channels to the plasma membrane in INS-832/13 cells (Wu et al., 2017). It is conceivable that, as in subthalamic neurons, Ca^{2+} influx through NMDA-gated channels activates K_{ATP} currents through a nitric oxide/cGMP-dependent pathway (Shen and Johnson, 2010). Hence, NMDAR activation seems to act as a negative feedback regulator for glucose-

induced insulin secretion by promoting K^+ outward currents, which initiate repolarization of the membrane potential. Marquard *et al.* recommended DXM or rather its active metabolite dextrorphan (DXO) for treatment of type 2 diabetes mellitus because of its beneficial effects on insulin secretion (Marquard et al., 2015; Marquard et al., 2016, 2016). Direct effects on important steps of the stimulus-secretion coupling were accomplished with MK-801 (also known as dizocilpine), another noncompetitive NMDAR antagonist. MK-801 changed the pattern of glucose-induced Ca^{2+} oscillations in mouse islets, increased the plateau fraction of Ca^{2+} oscillations and prolonged the characteristic bursts of electrical activity in glucose-stimulated β-cells (Marquard et al., 2015). However, there is evidence that MK-801 not only blocks NMDAR but also interacts with voltage-dependent K^+ (K_v) channels. A direct inhibition of K_v channels was shown in dissociated sympathetic neurons and mesenteric arterial smooth muscle cells of rats (Wooltorton and Mathie, 1995; Kim et al., 2015). Several K_v channel subunits which exist in vascular smooth muscle cells are expressed in insulin-secreting cells (MacDonald and Wheeler, 2003). As repolarization of β-cell action potentials is mediated by activation of K_v channels (MacDonald and Wheeler, 2003), the above mentioned effects of MK-801 on Ca^{2+} oscillations might not only be based on interaction with the NMDAR. The aim of this work was to elucidate whether DXM and DXO, respectively, influence insulin secretion by affecting plasma membrane potential and cytosolic Ca^{2+} similar to MK-801. To further investigate whether the observed drug effects are attributable to inhibition of NMDAR and concomitant elimination of its negative feedback on the stimulus-secretion cascade or involve other mechanisms, it was tested whether the two compounds directly interact with K_{ATP} and/or L-type Ca^{2+} channels of primary mouse β-cells.

Methods

Cell and islet preparation

Experiments were performed with islets of Langerhans from adult male and female C57BL/6N mice (Charles River, Sulzfeld, Germany). The principles of laboratory animal care were followed according to German laws (Az. 53.5.32.7.1/MS-12668, health and veterinary office Münster, Germany). Breeding pairs of SUR1-KO mice (on a C57BL/6 background) as well as SUR1-KO islets for some initial experiments were kindly provided by Prof. Dr. Gisela Drews (Institute of Pharmacy, Department of Pharmacology and Clinical Pharmacy, University of Tübingen, Germany). Mice were euthanized using CO_2 and pancreatic islets of both genotypes were isolated similarly by collagenase digestion. Murine islets were dispersed to single cells by trypsin-EDTA treatment (0.25 %, 2 min). Islets or cells were cultured in RPMI 1640 medium (11.1 mM glucose) supplemented with 10 % fetal calf serum, 100 U/ml penicillin, and 100 µg/ml streptomycin at 37°C in 5 % CO_2 humidified atmosphere.

Solutions and chemicals

Electrophysiological measurements and recordings of $[Ca^{2+}]_c$ were performed with a bath solution of (in mM): 140 NaCl, 5 KCl, 1.2 $MgCl_2$, 2.5 $CaCl_2$, 10 HEPES, glucose as indicated, pH 7.4 adjusted with NaOH. For determination of Ca^{2+} currents the bath solution contained (in mM): 115 NaCl, 1.2 $MgCl_2$, 10 $CaCl_2$, 20 tetraethylammonium chloride (TEA), 10 HEPES, 15 glucose, 0.1 tolbutamide, pH 7.4 adjusted with NaOH. Pipette solution for recording of plasma membrane potential (V_m) consisted of (in mM): 10 KCl, 10 NaCl, 70 K_2SO_4, 4 $MgCl_2$, 2 $CaCl_2$, 10 EGTA, 5 HEPES, 0.27 amphotericin B, pH adjusted to 7.15 with KOH. For Ca^{2+} currents the pipette solution was composed of (in mM): 50 CsCl, 70 N-methyl-D-glucamin, 58 HCl, 4 $MgCl_2$, 2 $CaCl_2$, 10 EGTA, 3 Na_2ATP, 10 HEPES, pH adjusted to 7.15 with CsOH. To determine K_{ATP} currents, pipette solution was composed of (in mM): 130 KCl, 4 $MgCl_2$, 2 $CaCl_2$, 10 EGTA, 0.65 Na_2ATP and 20 HEPES, pH 7.15 adjusted with KOH. Krebs-Ringer-

HEPES solution (KRH) for insulin secretion was composed of (in mM): 122 NaCl, 4.7 KCl, 1.1 $MgCl_2$, 2.5 $CaCl_2$, 10 HEPES, glucose as indicated, 0.5 % bovine serum albumin (BSA) and pH 7.4 adjusted with NaOH.

Dextromethorphan hydrobromide was obtained from Alfa Aesar (Thermo Fisher, Karlsruhe, Germany), memantine hydrochloride from Fisher Scientific GmbH (Schwerte, Germany), Collagenase P from Roche Diagnostics (Mannheim, Germany), Corning® Matrigel® basement membrane preparation from VWR (Darmstadt, Germany), RPMI 1640, fetal calf serum and penicillin/streptomycin from Life Technologies (Darmstadt, Germany). Fura-2 acetoxymethylester (fura-2 AM) and rat insulin were ordered from Biotrend (Köln, Germany). Dextrorphan tartrate and all other chemicals were from Sigma-Aldrich (Taufkirchen, Germany) or Diagonal (Münster, Germany).

Insulin secretion

After preparation, islets were kept overnight in RPMI medium. The next day, medium was removed and islets were incubated in KRH with 5.6 mM glucose for 1 h and thereafter in KRH buffer with 3 mM glucose for 0.5 h. In case of pre-incubation, the compounds were already added to the KRH buffer containing 5.6 mM and 3 mM glucose. For determination of insulin secretion, batches of five islets were incubated at 37°C for 60 min with the indicated substances and glucose concentrations. Each condition was prepared in triplicate. For analysis of the kinetics of insulin release, bath chambers were equipped with 50 islets and perfused with KRH at the indicated conditions at a rate of 0.7 ml/min at 37°C. Eluate samples were taken every 2 min. Insulin concentration was quantified by a radioimmunoassay using rat insulin as standard. In perfusion experiments, the substimulatory phase was evaluated by determining the area under the curve (AUC) of a 15-minute time interval. For analysis of glucose-stimulated secretion, the AUC was calculated starting from the first rise in insulin release after changing glucose concentration to 15 mM until the end of the experiment (approximately 50 min).

JPET Fast Forward. Published on July 14, 2020 as DOI: 10.1124/jpet.120.265835
This article has not been copyedited and formatted. The final version may differ from this version.

Measurement of $[Ca^{2+}]_c$

For determination of $[Ca^{2+}]_c$, islets were cultured for 1-2 d on glass coverslips coated with poly-L-lysine. Islets were loaded with fura-2 AM (5 μM, 37°C, 30 min) and thereafter perfused with bath solution plus indicated test substances. Fluorescence was excited at 340 nm and 380 nm and emission was measured by a digital camera (filter 515 nm). Alterations in mean $[Ca^{2+}]_c$ were evaluated by calculating the average of the mean Ca^{2+} concentration in bath solution with 3 or 8 mM glucose for 15 minutes (1 h pre-incubation experiments), for the last 5 minutes with the respective test compounds (acute application) or for the last 2 minutes in the presence of 0.5 mM glucose. The effect of DXM on the interburst duration was calculated by averaging the two preceding interburst intervals under control conditions in comparison to the period where $[Ca^{2+}]_c$ remained at the basal niveau after addition of DXM. To confirm that the islets were metabolically intact bath solution with 0.5, or 8 mM glucose was applied at the end of each experiment. Pancreatic β-cells exhibit characteristic glucose-evoked oscillations, which disappear in the presence of a low glucose concentration (Grapengiesser et al., 1988).

Electrophysiology

Patch-clamp experiments were performed with single islet cells. Pipettes were pulled from borosilicate glass capillaries (resistance of 3-5 MΩ). An EPC-10 patch-clamp amplifier (HEKA, Germany, software “Patchmaster” and “Fitmaster”) was used for data acquisition and analysis. V_m was measured in the current clamp mode. V_m was evaluated by determination of the plateau potential (from which action potentials start) for a period of 1 min before changing bath solution. The frequency of action potentials was evaluated during a 4- to 5-minute interval. K_{ATP} current was recorded by application of 300 ms pulses to -80 and -60 mV, respectively, starting from a holding potential of -70 mV every 15 s. K_{ATP} current was determined for the voltage step from -70 to -60 mV. Ca^{2+} current was recorded by 3 repetitive 100 ms pulses to 0 mV in 3-second intervals, starting from a holding potential of -70 mV every 30 s. The peak

Ca^{2+} current was analyzed and the currents of 3 succeeding pulses for each measuring point were averaged. For voltage-clamp experiments cells were identified as β-cells by glucose-dependent appearance of action potentials (see $[Ca^{2+}]_c$ experiments). In current measurements we used the cell capacitance as a criterion for β-cell identification (Göpel et al., 1999). The mean cell capacitance of all cells selected for analysis was 8±2 pF.

Electrical activity of whole islets was determined by extracellular membrane potential recordings with microelectrode arrays (MEA2100-system with 60MEA200/30iR-Ti-gr and MC-Rack software, Multi Channel Systems, Reutlingen, Germany). Data were low-pass filtered at 25 Hz and sampled at 1000 Hz. Islets were cultured for 3 to 4 days on microelectrode arrays (MEAs) coated with Matrigel®. Medium was changed to bath solution with 3 mM glucose at the beginning of each experiment. Thereafter, glucose was elevated to 8 mM, followed by addition of test compounds as indicated. For analysis, the fraction of plateau phase (FOPP, i.e. time with bursting activity related to the entire time interval) was calculated at the end of each experimental maneuver for a period of 20 min. Differences in sample sizes are due to the random number of islets attaching on an electrode of the microelectrode array.

Statistics

Data were collected from islets or islet cells of at least three independent mouse preparations for each series of experiments. Values are given as scatter plots and means ± SD. Data were normally distributed. Statistical significance was assessed by unpaired Student's t-test (Fig. 2 and 3D), paired Student's t-test (Fig. 3F, 4B, 4D, 5B, 5G, and 6C) or by ANOVA followed by Student-Newman-Keuls *post hoc* test for multiple comparisons (Fig. 1, 3B, 4C, 5D, 5E and 6A). The null hypothesis of each series of experiments was that the test compound has no influence on the respective parameter. Values of $p \leq 0.05$ were considered as statistically significant.

Results

DXM and DXO increase insulin secretion

The influence of the NMDAR antagonists DXM and its metabolite DXO on insulin secretion was investigated in the presence of different glucose concentrations. Islets incubated with 100 µM DXM for 1 h secreted significantly more insulin during stimulation with 3, 8, 10, or 15 mM glucose compared to control (Fig.1A). The same effect was evoked by 100 µM DXO, but to achieve this, the incubation time had to be elevated from 1 to 2.5 h. Most likely, this is due to the higher hydrophilicity of the demethylated compound (Yu and Haining, 2001). In these experiments, islets were already treated with DXO after changing the culture medium (10 mM glucose) to KRH solution with substimulatory glucose concentrations for 1.5 h prior to the 1-h stimulation with glucose (Fig 1B). Neither DXM nor DXO enhanced significantly glucose-stimulated insulin secretion at a lower concentration of 10 µM (Fig. 1C and D). Basal insulin release was also unaffected by this concentration (3 mM glucose control: 0.07±0.02 ng insulin/(islet*h), + 10 µM DXM: 0.06±0.03 ng insulin/(islet*h), n=6, p=0.6, + 10 µM DXO: 0.056±0.006, n=6, p=0.1). Strikingly and in contrast to DXO, insulin release was even reduced by around 40 % by DXM at a concentration of 500 µM (Fig.1C). As 100 µM DXO and DXM, respectively, stimulated insulin secretion most efficiently in our experiments, we further evaluated how the kinetics of insulin secretion were affected by this concentration. Glucose induces insulin secretion in a biphasic pattern: an initial peak (first phase), which develops rapidly but lasts only a few minutes, followed by a persistent plateau (second phase). DXO and DXM influenced both phases of glucose-induced insulin release. Similar to the effect in static incubations, both compounds substantially elevated insulin secretion at 3 mM glucose (Fig. 1 E).

Influence of NMDAR antagonists on membrane potential oscillations

NMDARs are ligand- and voltage-gated ion channels, which allow the permeation of Ca^{2+} ions. As changes in membrane potential and subsequent Ca^{2+} influx are the key events for regulation of insulin release, we studied the influence of the NMDAR antagonists on electrical activity. Whole pancreatic islets were cultured for 3 to 4 days on microelectrode arrays to achieve a close contact between islet and electrode. The fraction of plateau phase (FOPP), i. e., the period islets display bursts of action potentials, was determined at a glucose concentration of 8 mM, which is close to the threshold concentration for activation of mouse islets. At this glucose concentration, the FOPP varied around 10 to 20 % and stimulatory effects were easy to detect. The oscillatory pattern induced by 8 mM glucose was changed to permanent depolarization after application of 100 µM DXM (representative experiment shown in Fig. 2A, lower trace). Corresponding to the results observed for insulin secretion, the low concentration of 10 µM DXM elevated the FOPP significantly less than 100 µM DXM (Fig. 2A upper trace, Fig. 2B evaluation of all recordings). Similar results were obtained for DXO (Fig. 2C, D).

Effects of DXM and DXO on $[Ca^{2+}]_c$ in islets and single β-cells

So far, our data support the hypothesis concluded from the experiments with MK-801 (Marquard et al., 2015) that blocking NMDAR augments the glucose-induced depolarization of β-cells. As this is expected to result in a rise in Ca^{2+} influx, we examined if changes in electrical activity and glucose-induced insulin secretion are correlated to changes in $[Ca^{2+}]_c$. Treatment of whole islets with DXM (100 µM) abolished the typical oscillatory pattern of $[Ca^{2+}]_c$ in the presence of 8 mM glucose and elevated $[Ca^{2+}]_c$ compared to controls (Fig. 3A lower vs. upper part, evaluation of all experiments: Fig. 3B). In these experiments, DXM was added to the bath solution 1 h before and during the initial part of the recording. Of note, $[Ca^{2+}]_c$ further increased directly after wash-out of DXM and sometimes fast oscillations reoccurred. Furthermore, analysis of basal $[Ca^{2+}]_c$ at the end of each experiment, where glucose concentration was

lowered from 8 to 0.5 mM, revealed that $[Ca^{2+}]_c$ decreased as expected, but remained on a higher level in those islets exposed to DXM before compared to controls (Fig. 3B). To test whether DXM elevates $[Ca^{2+}]_c$ at a substimulatory glucose concentration, it was added in the presence of 3 mM glucose for 1 h. Thereafter, the recording was started and $[Ca^{2+}]_c$ was monitored for 15 min with DXM still present (see Fig. 3C, lower trace). This maneuver was followed by the wash-out of DXM and finally by switching glucose concentration from 3 to 8 mM to confirm the metabolic integrity of the islets. Evaluation of these data showed that DXM increased the basal $[Ca^{2+}]_c$ (Fig. 3D). Another series of experiments revealed that basal $[Ca^{2+}]_c$ increased in response to acute treatment with DXM (15 min) but the effect was much less pronounced (3 mM glucose: $F_{340/380}$: 0.48±0.10 a. u., + 100 µM DXM: 0.50±0.11 a. u., n=8, p=0.04, data not shown).

Next, we investigated the acute influence of DXM on $[Ca^{2+}]_c$ in glucose-stimulated islets. Remarkably, DXM (100 µM, 10 min) exerted a dual effect on the Ca^{2+} oscillations triggered by 8 mM glucose. Initially, the time $[Ca^{2+}]_c$ remained at the low "interburst" level was prolonged. This was observed consistently: when DXM was added at the beginning, on top of or at the end of an oscillation. Thereafter, $[Ca^{2+}]_c$ raised to a plateau with or without small, superimposed oscillations, whereas regular, large oscillations did not reoccur during the application of DXM (Fig. 3E, upper trace). For analysis of the initial effect of DXM the interburst interval of the glucose-induced oscillations was calculated and compared to the time $[Ca^{2+}]_c$ dropped to the interburst niveau in response to DXM. This period was considerable elevated (control 1.1±0.5 min *vs.* DXM 3.4±0.9 min, n=14, p=0.000001). Evaluation of the last 5 minutes of drug application showed that, similar to the results obtained with pre-incubated islets, mean $[Ca^{2+}]_c$ was increased in DXM-treated cells *vs.* control (Fig. 3F, left part).

Analogous experiments were performed with DXO. Acute application of 100 µM DXO to islets stimulated by 8 mM glucose slightly elevated mean $[Ca^{2+}]_c$ (Fig. 3E, lower trace and Fig. 3F,

right part), but the effect was substantially lower compared to DXM (last 5 min of application of DXO: 1.1±0.2 a. u., n=17 *vs.* DXM 1.3±0.2 a. u., n=14, p=0.0003). In contrast to DXM, DXO did not prolong the first interburst phase after drug application.

Opposing effects of DXM and DXO on membrane potential in single β-cells

The transient inhibition of Ca^{2+} oscillations in response to acute application of DXM was unexpected, as inhibition of NMDAR should dampen the negative feedback of Ca^{2+}-dependent activation of repolarizing currents. Therefore, the influence of DXM on Ca^{2+} action potentials and ion channels was investigated in patch-clamp experiments. In the perforated-patch configuration where cell metabolism is intact, application of DXM (100 µM) to β-cells stimulated by 8 mM glucose led to an initial reduction in the frequency of action potentials (Fig. 4A, B). β-cells were hyperpolarized in 1 out of 6 experiments, but overall, V_m was unaffected (control -35±7 mV *vs.* DXM -31±6 mV, n=6, p=0.11). The inhibiting effect of 100 µM DXM was also present at a glucose concentration of 15 mM. The lower concentration of 10 µM DXM did not affect action potential frequency (Fig. 4C). In agreement with the Ca^{2+} data there was no negative effect of 100 µM DXO on Ca^{2+} action potentials (Fig. 4D). In summary, these data suggest a direct interaction of DXM with other ion channels apart from NMDAR, e. g. L-type Ca^{2+} channels.

Influence on Ca^{2+} and K_{ATP} current

To test for direct interactions of the NMDAR antagonists with other ion channels, patch-clamp experiments were performed in the whole-cell configuration, where cell metabolism is disrupted. The currents were identified as Ca^{2+} currents by application of the L-type Ca^{2+} channel inhibitor nifedipine (10 µM) (Rorsman and Trube, 1986) in each measurement. In agreement with a drop in $[Ca^{2+}]_c$, DXM (100 µM) partially inhibited the Ca^{2+} current (Fig. 5A, B). Besides a reduction in peak current (Fig. 5B), the decay of the current tended to be faster

after application of DXM. This might indicate an influence on channel inactivation (decay time to 63 % of the peak current, control: 40±24 ms, n=4, + DXM: 29±13 ms, n=5, p=0.39).

As this result could not explain why the Ca^{2+}-lowering effect was only transient, it was investigated whether DXM also interacts with K_{ATP} channels. It was described that NMDA receptor activity contributes to K_{ATP} channel trafficking and activity but up to now there is no information about any direct effects of NMDAR blockers on this ion channel (Shen and Johnson, 2010; Wu et al., 2017). Both compounds, DXM and DXO, inhibited the K_{ATP} current (Fig. 5C-F). DXM reduced the K_{ATP} current dose-dependently (Fig. 5C, D). The effect was statistically significant at 50 µM (control: 20±5 pA/pF *vs.* DXM 50 µM: 16±5 pA/pF, n=6, p=0.0007) and 100 µM (control: 24±5 pA/pF *vs.* DXM 100 µM: 7±4 pA/pF, n=5, p=0.001). After withdrawal of DXM (100 µM) there was a partial recovery in 2 out of the 5 experiments and, on average, K_{ATP} current rose to 12±4 pA/pF (n=5, p=0.23 *vs.* DXM). The inhibitory effect of DXM was not antagonized by 100 µM diazoxide (Fig. 5E) (Dabrowski et al., 2003). DXO (100 µM) also lowered the K_{ATP} current to more than 50 % of control (Fig. 5F, G). This effect was not reversible (8±5 pA/pF, n=5, p=0.36 *vs.* DXO). Currents were identified as K_{ATP} currents by application of tolbutamide (100 µM) (Trube et al., 1986) in each recording. To elucidate, whether direct inhibition of K_{ATP} channels is a side-effect shared by other NMDAR blockers, memantine was tested. K_{ATP} current was reduced to approximately 30 % by 100 µM of this drug (Suppl. Fig. 1).

Contribution of K_{ATP} channels to the rise in insulin secretion by DXM and DXO

The data described above show that DXM and DXO directly influence K_{ATP} and Ca^{2+} channels in addition to their well-known function as NMDR antagonists. To investigate the significance of inhibition of K_{ATP} and/or L-type Ca^{2+} channels for modulation of insulin release we used islets of SUR1 knockout (SUR1-KO) mice that do not express functional K_{ATP} channels in their plasma membrane (Seghers et al., 2000). Insulin secretion of SUR1-KO islets stimulated by 15

mM glucose was not elevated by 100 µM DXM (Fig. 6A). $[Ca^{2+}]_c$ measurements with SUR1-KO islets even showed a substantial decrease in mean $[Ca^{2+}]_c$ when DXM was added to the bath solution (Fig. 6B, upper graph and Fig. 6C, left). This loss of stimulatory effects in SUR1-KO islets demonstrates that inhibition of K_{ATP} channels is the underlying mechanism for the elevation of insulin release by DXM. In comparison, DXO clearly tended to rise insulin secretion in SUR1-KO islets when stimulated with 15 mM glucose (Fig. 6A, hatched bar). In addition, determination of the acute effect of DXO on $[Ca^{2+}]_c$ in SUR1-KO islets revealed a slight, but statistically significant increase by 100 µM DXO (Fig. 6B lower graph, and Fig. 6C, right). These data suggest that additional, K_{ATP} channel-independent pathways contribute to the insulinotropic effect of DXO.

Discussion

DXM and DXO can increase glucose-induced insulin secretion and were proposed to be potential drugs for treatment of type 2 diabetes mellitus. How NMDAR might modulate β-cell function was investigated with MK-801 (Marquard et al., 2015). Controversial results exist regarding the effect of this compound on insulin release. While one group (Marquard et al., 2015) detected an elevation of glucose-stimulated insulin secretion, others describe no effect during acute application of MK-801 (Bertrand et al., 1992; Chan et al., 1997; Patterson et al., 2016), or even inhibition after prolonged exposure (Patterson et al., 2016). Consequently, it is difficult to conclude from experiments with MK-801 to the mode of action of DXM and DXO. Our results reveal that DXM and its metabolite DXO elevate electrical activity, $[Ca^{2+}]_c$ and insulin secretion. The most efficient concentration in our experiments was 100 µM. This concentration will certainly not be reached in the plasma but cumulative effects might occur in tissues during long-term use. 10 µM DXO led to inconclusive results in our study: A rise in secretion was observed in 2 out of the 6 mouse preparations, whereas the others showed no or only a negligible response. This result contrasts to Marquard *et al.* (Marquard et al., 2015) and cannot not be explained by differences in methodology. Of note, Suwandhi *et al.* (Suwandhi et al., 2018) describe a clear stimulatory trend for 10 µM DXO but also no significant effect.

At first glance, our data support the hypothesis, that NMDAR antagonists enhance insulin release via the triggering pathway, regulated by the plasma membrane potential. Mechanistically, the NMDAR can interact with insulin secretion by several pathways. Wu *et al.* reported increased trafficking of K_{ATP} and $K_V2.1$ channels to the membrane surface in response to NMDA (Wu et al., 2017). The rise in Ca^{2+} influx via NMDAR could also depolarize mitochondria thereby increasing the open probability of K_{ATP} channels, as described for Ca^{2+}-influx via voltage-regulated Ca^{2+} channels (Ca_v channels) (Drews et al., 2015). Finally, increased local $[Ca^{2+}]_c$ could activate Ca^{2+}-regulated K^+ channels (K_{Ca} channels). Together

with the hyperpolarizing current through K_{ATP} channels, opening of K_{Ca} channels is known to initiate the end of each burst phase during the typical oscillations of glucose-stimulated pancreatic islets (Düfer et al., 2009; Rorsman and Ashcroft, 2018). Consequently, inhibition of NMDARs should impede repolarization of the β-cell and prolong the burst phases of electrical activity. For MK-801 it was suggested that the stimulatory effect requires K_{ATP} channels (Marquard et al., 2015). To elucidate whether this also applies to DXM and DXO, islets of SUR1-KO mice were used. The two NMDAR antagonists acted differently in K_{ATP}-channel deficient islets. Concomitant with the loss of any positive influence on $[Ca^{2+}]_c$, insulin release was not stimulated by DXM in SUR1-KO islets. By contrast, DXO still elevated $[Ca^{2+}]_c$, although the effect was less pronounced compared to wildtype islets. The effect of DXO on insulin release was more variable in SUR1-KO islets. Stimulation was observed in 7 out of 10 experiments. Statistical significance was reached when tested separately *vs.* control by a Student´s t-test but not in the ANOVA group comparison.

So far, it is obvious that K_{ATP} channels play a central role for the efficacy of DXM and – together with other mechanisms – are involved in the mode of action of DXO. To clarify whether NMDAR is the predominant target for modulation of K_{ATP} channel activity, we investigated the direct influence on other ion channels. Our experiments show for the first time that DXM and DXO both directly inhibit K_{ATP} channels. The effect of DXM was resistant to diazoxide. This differs from the characteristics of established K_{ATP} channel blockers (Rorsman and Trube, 1986) but was reported, e. g., for the experimental compound phentolamine (Plant and Henquin, 1990). As the K_{ATP} channel blockade was very fast and strong, we assume that this direct interaction is much more important for β-cell stimulation than indirect pathways induced by inhibition of NMDAR. Direct inhibition of K^+ currents by DXM was reported for $K_v1.3$ channels (Lee et al., 2011). These channels seem to be irrelevant for glucose-stimulated insulin secretion but are associated with regulation of insulin sensitivity (Choi and Hahn, 2010).

Taken together, DXM may improve glycemic control by a dual mechanism: an increase in insulin sensitivity and a rise in insulin secretion. In principle, such a combination is not bad, but direct block of K_{ATP} channels in β-cells always bears the risk of hypoglycemia. This apprehension is supported by results of Suwandhi *et al.* showing a statistically significant membrane depolarization of β-cells with DXO at 2 mM glucose (Suwandhi et al., 2018) and by our observation that DXO and DXM extremely elevate insulin release in the presence of 3 mM glucose. DXO stimulates insulin release at this low glucose concentration but is most effective in the presence of 8, and 10 mM glucose. This is in line with a compound inhibiting K_{ATP} channels. At 15 mM glucose, when the majority of K_{ATP} channels is already closed, the effect of channel blockers (sulfonylureas or glinides) is less pronounced (Joost and Hasselblatt, 1979; Ikenoue et al., 1997), similar to our results with DXO.

Apart from the problem of nutrient-independent insulin release, limiting the therapeutic potential of DXM and DXO equally, our study revealed a Ca^{2+}-lowering effect of DXM. The drop in $[Ca^{2+}]_c$ was relatively short and transient in wildtype islets but persisted during the whole application period in SUR1-deficient islets. As this is neither compatible with direct inhibition of K_{ATP} channels nor with interruption of the indirect negative feedback via NMDAR and K_{ATP} or K_{Ca}-channels, DXM must address an additional target. Indeed, we could show that DXM reduces the peak current through L-type Ca^{2+} channels. Inhibition of Ca_v channels by DXM (and DXO) was described for neuronal cells (Carpenter et al., 1988; Netzer et al., 1993). Our patch-clamp recordings, where intracellular Ca^{2+} was clamped to a low level, suggest an accelerated inactivation by this compound, but further studies are necessary to address this point in detail. Affinity assays showed a 10-fold higher affinity to Ca_v channels for DXM *vs.* DXO. Furthermore, the affinity of DXM to Ca_v channels is 1.7-fold higher than to NMDARs (Jaffe et al., 1989). In agreement with this differences in the inhibitory potencies, DXM lowered the frequency of Ca^{2+} action potentials in patch-clamped β-cells, whereas DXO neither affected

JPET Fast Forward. Published on July 14, 2020 as DOI: 10.1124/jpet.120.265835
This article has not been copyedited and formatted. The final version may differ from this version.

action potentials nor reduced $[Ca^{2+}]_c$. In SUR1-KO islets DXM lowered $[Ca^{2+}]_c$ but the remaining level was still above basal and glucose-stimulated insulin release was not negatively affected. Of note, the high concentration of 500 µM DXM dramatically decreased glucose-stimulated insulin release of wildtype islets. This suggests that the inhibitory effect on L-type Ca^{2+} channels outweighs all other signaling pathways DXM acts on when the drug accumulates in pancreatic tissue or is severely overdosed.

DXM and DXO also differ in their ability to bind to NMDAR: The affinity of DXO to the NMDAR was reported to be 6.5 times higher compared to DXM (Jaffe et al., 1989) and in contrast to DXM, DXO still raised $[Ca^{2+}]_c$ in SUR1-KO islets. This provides evidence for the potential of NMDAR antagonists to improve β-cell function apart from any (direct or indirect) interaction with K_{ATP} channels. Reduced activation of K_{Ca} channels might play an important role in this scenario. NMDA receptors couple to or are part of a Ca^{2+}-mediated feedback loop with K_{Ca} channels in neurons (Isaacson and Murphy, 2001; Ngo-Anh et al., 2005). One candidate might be the SK4 channel (syn. $K_{Ca}3.1$ channel) which is known to be part of the slowly rising K^+ currents terminating burst phases in oscillating β-cells. Eliminating this component of the so-called K_{slow} current dampens the negative feedback mechanisms maintaining oscillations and elevates $[Ca^{2+}]_c$, thereby fostering insulin release (Düfer et al., 2009). Targeting this pathway has the big advantage that it is not operative under basal $[Ca^{2+}]_c$, i.e. without nutrient stimulation. In this context, it is astonishing why blocking NMDAR by MK-801 was completely ineffective in Kir6.2-KO islets (Marquard et al., 2015). Possibly, loss of K_{ATP} channels affects the alternative pathways recruited to preserve glucose-regulated hormone secretion differently in the two mouse models. This assumption is supported by the observation that insulin release of islets of Kir6.2-KO mice is less sensitive glucose (Miki et al., 1998; Marquard et al., 2015) compared to islets of SUR1-KO mice (Fig. 6 and (Haspel et al., 2005)). Furthermore, it was shown for β-cells of SUR1-KO mice that K_{Ca} channels could

be activated by forced Ca^{2+}-influx (Haspel et al., 2005), but it is not known whether this also applies to Kir6.2-deficient β-cells.

DXM was already tested in combination with sitagliptin in a small clinical trial. DXM (independent of dose) numerically reduced maximum blood glucose concentration in response to an oral glucose tolerance test (Marquard et al., 2016). Although the effect was not statistically significant, the results may encourage people to use DXM as an oral antidiabetic drug. Strikingly, development of insulin-dependent diabetes mellitus was reported in a pilot study investigating the therapeutic potential of DXM for treatment of children with severe meningitis (Konrad et al., 2000). With respect to the risk of negative side effects, one can argue that DXO, as the main active metabolite, would be the leading compound reaching the endocrine pancreas. However, it is well known that metabolism of DXM is variable and can occur incomplete. As DXM is metabolized to DXO by CYP2D6 (Yu and Haining, 2001) it accumulates in people with CYP2D6 deficiency due to genetic polymorphisms. A study with 12 healthy volunteers revealed, that after ingestion of 25 mg of DXM, the plasma samples of 3 volunteers contained exclusively DXM and in another 3 volunteers low concentrations of un-metabolized DXM could still be detected (Pfaff et al., 1983). These data underline the unpredictability of metabolism-related drug effects in patients with unknown CYP2D6 status or in patients receiving any CYP2D6 inhibiting drugs.

In summary, our data indicate that NMDAR influences glucose-mediated stimulus-secretion coupling by K_{ATP} channel-dependent and -independent pathways. With respect to DXM and DXO the stimulatory mode of action is rather based on direct inhibition of K_{ATP} channels than on NMDAR blockade. To investigate the role of NMDAR in β-cell (patho)physiology and to further elucidate the therapeutic potential of NMDAR inhibitors, novel compounds that, e. g., specifically target NMDAR subunits or are unrelated to the morphinan core structure, have to be developed.

Acknowledgments

We thank Julia Kaiser and Jelena Sikimic for preparation of SUR1-KO islets and Melanie Arning and Katrin von Schroetter for skillful technical assistance.

Author contributions

Participated in research design: Gresch, Düfer

Conducted experiments: Gresch

Performed data analysis: Gresch

Wrote or contributed to the writing of the manuscript: Gresch, Düfer

Conflict of interests

The authors declare no conflict of interests.

References

Bertrand G, Gross R, Puech R, Loubatières-Mariani MM, and Bockaert J (1992) Evidence for a glutamate receptor of the AMPA subtype which mediates insulin release from rat perfused pancreas. *Br. J. Pharmacol.* **106:**354–359.

Carpenter CL, Marks SS, Watson DL, and Greenberg DA (1988) Dextromethorphan and dextrorphan as calcium channel antagonists. *Brain Res.* **439:**372–375.

Chan SLF, Pallett AL, Clews J, Ramsden CA, and Morgan NG (1997) Evidence that the ability of imidazoline compounds to stimulate insulin secretion is not due to interaction with σ receptors. *Eur. J. Pharmacol.* **323:**241–244.

Choi BH and Hahn SJ (2010) Kv1.3: A potential pharmacological target for diabetes. *Acta Pharmacol. Sin.* **31:**1031–1035.

Dabrowski M, Larsen T, Ashcroft FM, Bondo Hansen J, and Wahl P (2003) Potent and selective activation of the pancreatic beta-cell type K(ATP) channel by two novel diazoxide analogues. *Diabetologia* **46:**1375–1382.

Drews G, Krippeit-Drews P, and Düfer M (2015) Electrophysiology of Islet Cells, in *Islets of Langerhans*, 2nd ed. 2015 (Islam MS ed) pp 249–303, Springer Netherlands, Dordrecht.

Düfer M, Gier B, Wolpers D, Krippeit-Drews P, Ruth P, and Drews G (2009) Enhanced glucose tolerance by SK4 channel inhibition in pancreatic β-cells. *Diabetes* **58:**1835–1843.

Gonoi T, Miszuno N, Inagaki N, Kuromi H, Seino Y, Miyazaki J-i, and Seino S (1994) Functional neuronal ionotropic glutamate receptors are expressed in the non-neuronal cell line MIN6. *J. Biol. Chem.* **269:**16989–16992.

Göpel S, Kanno T, Barg S, Galvanovskis J, and Rorsman P (1999) Voltage-gated and resting membrane currents recorded from B-cells in intact mouse pancreatic islets. *J. Physiol.* **521.3:**717–728.

Grapengiesser E, Gylfe E, and Hellman B (1988) Glucose-induced oscillations of cytoplasmic Ca^{2+} in the pancreatic β-cell. *Biochem. Biophys. Res. Commun.***151:**1299–1304.

Haspel D, Krippeit-Drews P, Aguilar-Bryan L, Bryan J, Drews G, and Düfer M (2005) Crosstalk between membrane potential and cytosolic Ca^{2+} concentration in beta cells from $Sur1^{-/-}$ mice. *Diabetologia* **48:**913–921.

Ikenoue T, Akiyoshi M, Fujitani S, Okazaki K, Kondo N, and Maki T (1997) Hypoglycaemic and insulinotropic effects of a novel oral antidiabetic agent, (-)-N-(trans-4-isopropylcyclohexanecarbonyl)-D-phenylalanine (A-4166). *Br. J. Pharmacol.* **120:**137–145.

Imai R, Misaka S, Horita S, Yokota S, O'hashi R, Maejima Y, and Shimomura K (2018) Memantine has no effect on K_{ATP} channels in pancreatic β cells. *BMC Res. Notes* **11:**614.

Inagaki N, Kuromi H, Gonoi T, Okamoto Y, Ishida H, Seino Y, Kaneko T, Iwanga T, and Seino S (1995) Expression and role of ionotropic glutamate receptors in pancreatic islet cells. *FASEB J.* **9:**686–691.

Isaacson JS and Murphy GJ (2001) Glutamate-mediated extrasynaptic inhibition: Direct coupling of NMDA receptors to Ca^{2+}-activated K^+ channels. *Neuron* **31:**1027–1034.

Jaffe DB, Marks SS, and Greenberg DA (1989) Antagonist drug selectivity for radioligand binding sites on voltage-gated and *N*-methyl-D-aspartate receptor-gated Ca^{2+} channels. *Neurosci. Lett.* **105:**227–232.

Joost HG and Hasselblatt A (1979) Insulin release by tolbutamide and glibenclamide: A comparative study on the perfused rat pancreas. *Naunyn-Schmiedeberg's Arch. Pharmacol.* **306:**185–188.

Kim JM, Park SW, Lin HY, Shin KC, Sung DJ, Kim JG, Cho H, Kim B, and Bae YM (2015) Blockade of voltage-gated K^+ currents in rat mesenteric arterial smooth muscle cells by MK801. *J. Pharmcol. Sci.* **127:**92–102.

Konrad D, Sobetzko D, Schmitt B, and Schoenle EJ (2000) Insulin-dependent diabetes mellitus induced by the antitussive agent dextromethorphan. *Diabetologia* **43:**261–262.

Lee J-H, Choi S-H, Shin T-J, Lee B-H, Hwang S-H, Kim H-C, and Nah S-Y (2011) Effect of dextromethorphan on human $K_v1.3$ channel activity: Involvement of C-type inactivation. *Eur. J. Pharmacol.* **651:**122–127.

MacDonald PE and Wheeler MB (2003) Voltage-dependent K^+ channels in pancreatic beta cells: Role, regulation and potential as therapeutic targets. *Diabetologia* **46:**1046–1062.

Marquard J, Otter S, Welters A, Stirban A, Fischer A, Eglinger J, Herebian D, Kletke O, Klemen MS, Stožer A, Wnendt S, Piemonti L, Köhler M, Ferrer J, Thorens B, Schliess F, Rupnik MS, Heise T, Berggren P-O, Klöcker N, Meissner T, Mayatepek E, Eberhard D, Kragl M, and Lammert E (2015) Characterization of pancreatic NMDA receptors as possible drug targets for diabetes treatment. *Nat. Med.* **21:**363–372.

Marquard J, Stirban A, Schliess F, Sievers F, Welters A, Otter S, Fischer A, Wnendt S, Meissner T, Heise T, and Lammert E (2016) Effects of dextromethorphan as add-on to sitagliptin on blood glucose and serum insulin concentrations in individuals with type 2 diabetes mellitus: A randomized, placebo-controlled, double-blinded, multiple crossover, single-dose clinical trial. *Diabetes Obes. Metab.* **18:**100–103.

Miki T, Nagashima K, Tashiro F, Kotake K, Yoshitomi H, Tamamoto A, Gonoi T, Iwanga T, Miyazaki J-i, and Seino S (1998) Defective insulin secretion and enhanced insulin action in K_{ATP} channel-deficient mice. *Proc. Natl. Acad. Sci. USA* **95:**10402–10406.

Molnar E, Varadi A, McIlhinney RJ, and Ascroft SJH (1995) Identification of functional ionotropic glutamate receptor proteins in pancreatic β-cells and in islets of Langerhans. *FEBS Lett.* **371:**253–257.

Netzer R, Pflimlin P, and Trube G (1993) Dextromethorphan blocks N-methyl-D-aspartate-induced currents and voltage-operated inward currents in cultured cortical neurons. *Eur. J. Pharmacol.* **238:**209–216.

Ngo-Anh TJ, Bloodgood BL, Lin M, Sabatini BL, Maylie J, and Adelman JP (2005) SK channels and NMDA receptors form a Ca^{2+}-mediated feedback loop in dendritic spines. *Nat. Neurosci.* **8:**642–649.

Nguyen L, Thomas KL, Lucke-Wold BP, Cavendish JZ, Crowe MS, and Matsumoto RR (2016) Dextromethorphan: An update on its utility for neurological and neuropsychiatric disorders. *Pharmacol. Ther.* **159:**1–22.

Patterson S, Irwin N, Guo-Parke H, Moffett RC, Scullion SM, Flatt PR, and McClenaghan NH (2016) Evaluation of the role of N-methyl-D-aspartate (NMDA) receptors in insulin secreting beta-cells. *Eur. J. Pharmacol.* **771:**107–113.

Pfaff G, Briegel P, and Lamprecht I (1983) Inter-individual variation in the metabolism of dextromethorphan. *Int. J. Pharm.* **14:**173–189.

Plant TD and Henquin JC (1990) Phentolamine and yohimbine inhibit ATP-sensitive K^+ channels in mouse pancreatic β-cells. *Br. J. Pharmacol.* **101:**115-120.

Rorsman P and Ashcroft FM (2018) Pancreatic β-cell electrical activity and insulin secretion: of mice and men. *Physiol. Rev.* **98:**117–214.

Rorsman P and Trube G (1986) Calcium and delayed potassium currents in mouse pancreatic β-cells under voltage-clamp conditions. *J. Physiol.* **374:**531–550.

Seghers V, Nakazaki M, DeMayo F, Aguilar-Bryan L, and Bryan J (2000) *SUR1* Knockout Mice: A model for K_{ATP} channel-independent regulation of insulin secretion. *J. Biol. Chem.* **275:**9270–9277.

Shen K-Z and Johnson SW (2010) Ca^{2+} influx through NMDA-gated channels activates ATP-sensitive K^+ currents through a nitric oxide-cGMP pathway in subthalamic neurons. *J. Neurosci. Res.* **30:**1882–1893.

Suwandhi L, Hausmann S, Braun A, Gruber T, Heinzmann SS, Gálvez EJC, Buck A, Legutko B, Israel A, Feuchtinger A, Haythorne E, Staiger H, Heni M, Häring H-U, Schmitt-Kopplin P, Walch A, Cáceres CG, Tschöp MH, Rutter GA, Strowig T, Elsner M, and

Ussar S (2018) Chronic D-serine supplementation impairs insulin secretion. *Mol. Metab.* **16:**191–202.

Trube G, Rorsman P, and Ohno-Shosaku T (1986) Opposite effects of tolbutamide and diazoxide on the ATP-dependent K^+ channel in mouse pancreatic β-cells. *Pflügers Arch.* **407:**493–499.

Vyklicky V., Korinek M, Smejkalova T, Balik A, and Krausova B (2014) Structure, function, and pharmacology of NMDA receptor channels. *Physiol. Res.* **63:**191–203.

Wooltorton JRA and Mathie A (1995) Potent block of potassium currents in rat isolated sympathetic neurones by the uncharged form of amitriptyline and related tricyclic compounds. *Br. J. Pharmacol.* **116:**2191–2200.

Wu Y, Fortin DA, Cochrane VA, Chen P-C, and Shyng S-L (2017) NMDA receptors mediate leptin signaling and regulate potassium channel trafficking in pancreatic β-cells. *J. Biol. Chem.* **292:**15512–15524.

Yu A and Haining RL (2001) Comparative contribution to dextromethorphan metabolism by Cytochrome P450 isoforms in vitro: can dextromethorphan be used as a dual probe for both CYP2D6 and CYP3A activities? *Drug Metab. Dispos.* **29:**1514–1520.

Zhu S, Stein RA, Yoshioka C, Lee C-H, Goehring A, Mchaourab HS, and Gouaux E (2016) Mechanism of NMDA receptor inhibition and activation. *Cell* **165:**704–714.

Figure legends

Figure 1: Effects of DXM and DXO on insulin secretion of mouse islets. A) Acute treatment (1 h) with DXM (100 µM) elevates insulin release in the presence of 3, 8, 10 and 15 mM glucose. B) DXO (100 µM) induces stimulatory effects when exposure time was prolonged to 2.5 h (1.5 h pre-incubation and 1 h acute application). C) Insulin secretion (15 mM glucose) is not enhanced by 10 µM DXM but even reduced by 500 µM DXM. D) Islets stimulated with 15 mM glucose and treated with 10 µM DXO do not show enhanced insulin secretion. E) DXO and DXM elevate insulin release in the presence of 3 mM glucose and during the 1st and 2nd phase in response to stimulation with 15 mM glucose (evaluated areas marked in grey). The number of independent islet preparations from different mice is given below each bar. The diagrams in A) – E) summarize the results of all series. Islets were isolated from female/male mice as follows: 10/8 (A), 6/6 (B), 9/9 (C), 5/7 (D), 5/3 (E). *p≤0.05, **p≤0.01, ***p≤0.001 as indicated; # p≤0.05 *vs.* 10 mM glucose (A) and *vs.* 500 µM DXM (C); ### p≤0.001 *vs.* 15 mM glucose and all conditions with DXM (A, C), DXO (B, D); § p≤0.05 (A) and p≤0.001 (B) *vs.* 15 mM glucose. Please note: for clearness of presentation, only the most relevant significances are included in parts (A), (B) and (E) of this figure.

Figure 2: DXM and DXO increase the electrical activity of whole islets. A) Representative membrane potential recording of an islet cultured on a microelectrode array. Islets were stimulated with 8 mM glucose and acutely treated with DXM (10 µM upper trace, 100 µM lower trace). B) Evaluation of all experiments represented in (A). 100 µM DXM elevate the FOPP considerably more than 10 µM DXM. C) Same experimental setup as in (A, B) but with DXO instead of DXM. D) Acute application of DXO (100 µM) elevates the FOPP substantially more than 10 µM DXO. The number in brackets stands for the number of evaluated islets. Islets were isolated from female/male mice as follows: 3/0 (B), 3/0 (D). ***p≤0.001.

Figure 3: DXM increases $[Ca^{2+}]_c$ in whole islets. A) Representative recordings of $[Ca^{2+}]_c$ of an islet stimulated with 8 mM glucose alone (upper trace) or together with 100 µM DXM (lower trace). DXM was present 1 h before and during the experiment as indicated. B) Summary of all experiments represented in A. DXM elevates mean Ca^{2+} at 8 mM glucose in islets after 1 h pre-incubation. Basal Ca^{2+} evaluated at the end of each measurement is also elevated in islets pre-incubated with 100 µM DXM. C) DXM elevates mean Ca^{2+} at 3 mM glucose in islets after 1 h pre-incubation. D) Summary of all experiments presented in C. E) Representative recordings of $[Ca^{2+}]_c$ in islets stimulated with 8 mM glucose with acute application of 100 µM DXM (upper trace) or 100 µM DXO (lower trace). Compounds were added 15 min after starting the recording. F) Summary of all experiments represented in (E). Evaluation of the last 5 min of treatment with DXM shows a relevant increase of mean $[Ca^{2+}]_c$. Acute application of 100 µM DXO slightly elevates mean $[Ca^{2+}]_c$ of whole islets without an initial drop. The number of evaluated islets (B, D and F) is given below each data plot. Islets were isolated from female/male mice as follows: 1/2 (B), 1/2 (D), 2/4 (F). **p≤0.01, ***p≤0.001.

Figure 4: In contrast to DXO, DXM reduces Ca^{2+} action potentials in glucose-stimulated β-cells. A) Representative membrane potential recording of a pancreatic β-cell in the perforated-patch configuration. DXM (100 µM) decreases the frequency of action potentials (8 mM glucose). B) Summary of all experiments represented in (A). C) Summary of analogous experiments with 15 mM glucose. A lower concentration of DXM (10 µM) does not affect the number of Ca^{2+} action potentials. D) Similar experiments as in (A) but with DXO. 100 µM DXO have no effect on Ca^{2+} action potentials. The number in brackets represents the number of experiments with different cells from 3 mice. Islet cells were isolated from female/male mice as follows: 2/1 (B), 4/3 (C), 2/1 (D). *p≤0.05, **p≤0.01.

Figure 5: DXM acutely decreases Ca^{2+} peak currents and both compounds inhibit K_{ATP} channels of murine β-cells. A) Representative voltage-clamp recording in the whole-cell

configuration shows a decrease of the maximal Ca^{2+} current during administration of DXM (solid, black line) compared to control condition (solid, grey line). B) Summary of all experiments represented in (A). DXM (100 µM) reduces the Ca^{2+} current about 25 %. C, F) Representative recordings of K_{ATP} current measured in the whole-cell configuration. Administration of DXM (C) or DXO (F) directly decreases the K_{ATP} current. The current was identified as K_{ATP} current by the specific K_{ATP} channel inhibitor tolbutamide (100 µM). D) Dose-response curve for the direct effect of DXM (10, 20, 50 and 100 µM) on K_{ATP} current. Statistically significant inhibition occurred with 50 and 100 µM. E) Lack of antagonism of the DXM-induced inhibition by diazoxide (100 µM). G) Summary of all experiments with 100 µM DXO. The number in brackets indicates the number of experiments with different cells from 3 mice. Islet cells were isolated from female/male mice as follows: 4/1 (B), 7/3 (D), 0/3 (E), 3/0 (G) ~~(F)~~. *p≤0.05, **p≤0.01, ***p≤0.001 *vs.* all other conditions, #p≤0.05 *vs*. control and 20 µM DXM, ##p≤0.01 *vs*. control.

Figure 6: DXM and DXO affect $[Ca^{2+}]_c$ and insulin release differently in SUR1-KO islets. A) DXM (100 µM, 1.5 h pre-incubation and 1 h acute treatment) does not enhance insulin release (15 mM glucose) of murine SUR1-KO islets, while DXO (100 µM, 1.5 h pre-incubation and 1 h acute treatment) tends to have an elevating effect. B) Representative recordings of $[Ca^{2+}]_c$ of SUR1-KO islets stimulated with 8 mM glucose. The upper trace shows a drop in mean Ca^{2+} when DXM is added. By contrast, mean Ca^{2+} slightly rises after addition of DXO (lower trace). C) Summary of all experiments represented in (B). The numbers in brackets indicate independent islet preparations (A) or evaluated islets (C). Islets were isolated from female/male mice as follows: 6/4 (A), 5/2 (C). *p≤0.05, ***p≤0.001, ##p≤0.01 *vs.* 15 mM glucose, ###p≤0.001 *vs.* DXO and DXM.

Figure 1

Figure 2

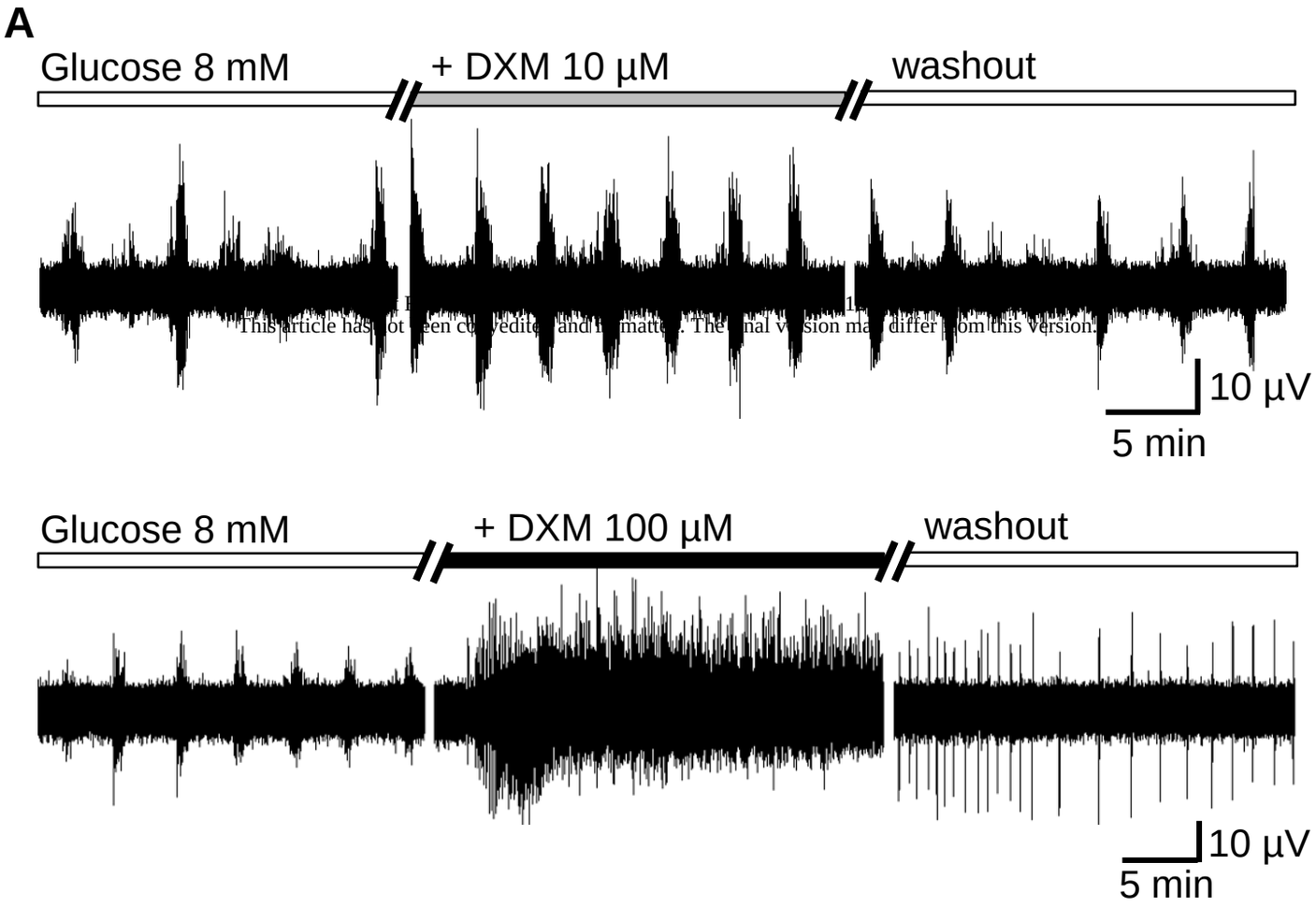

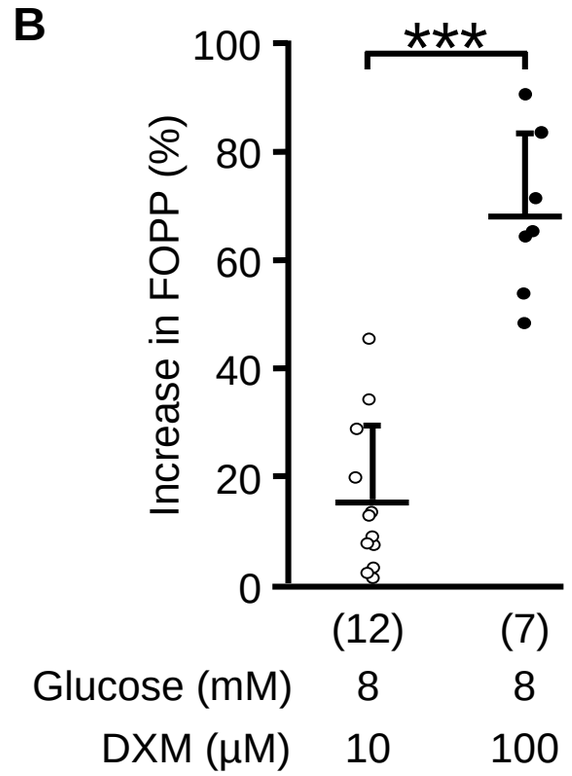

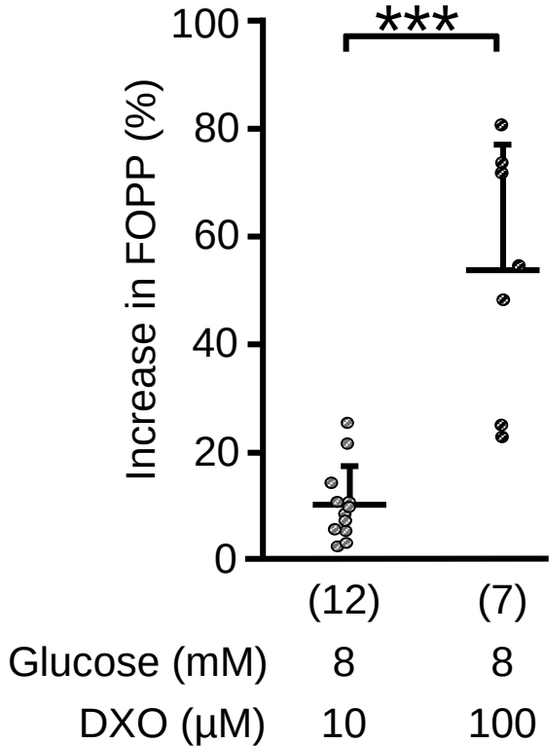

Figure 3

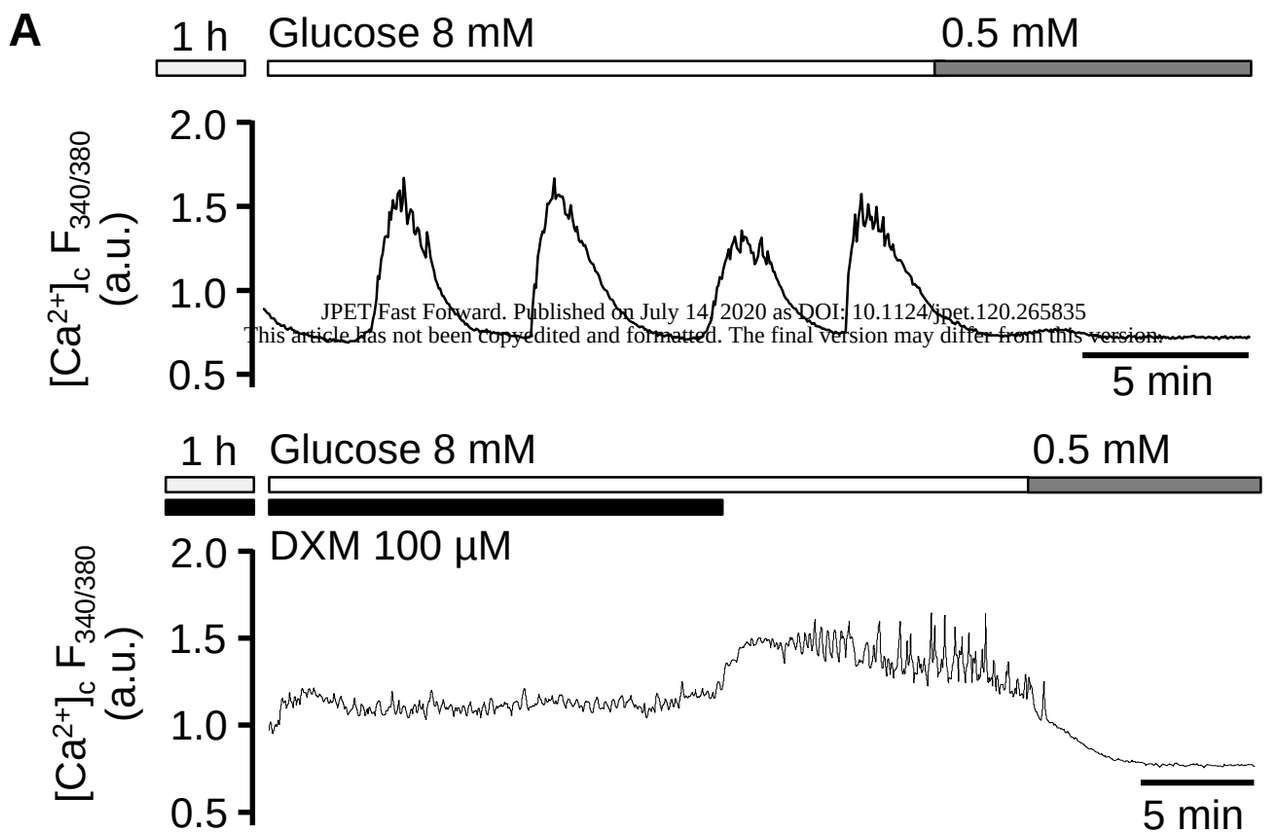

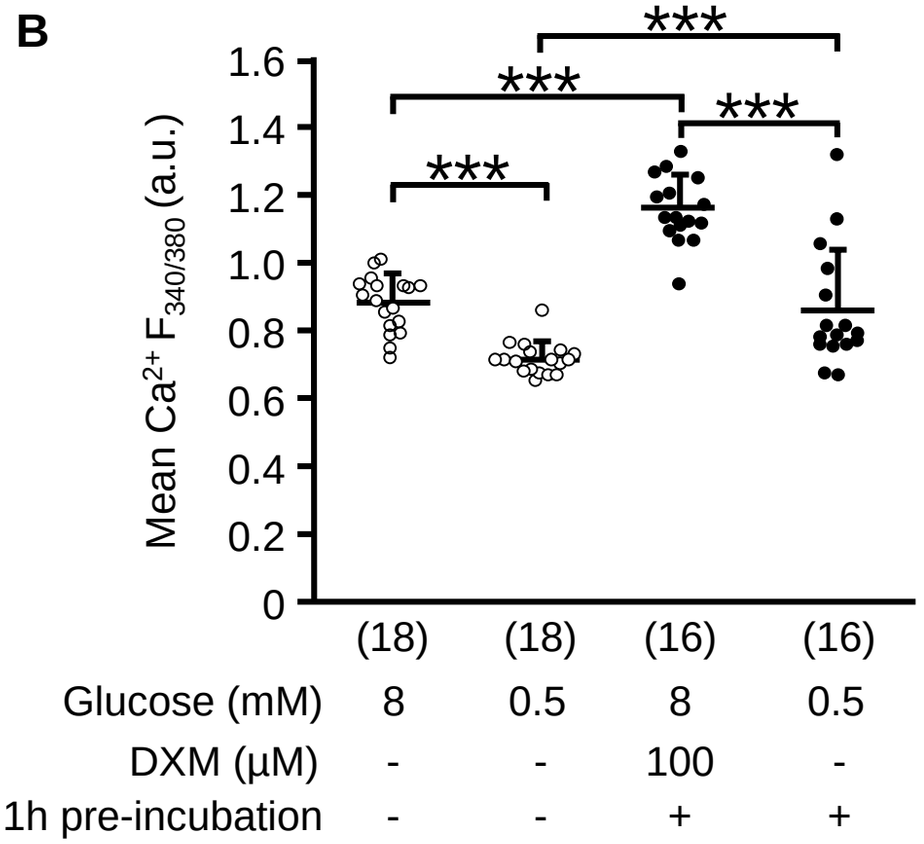

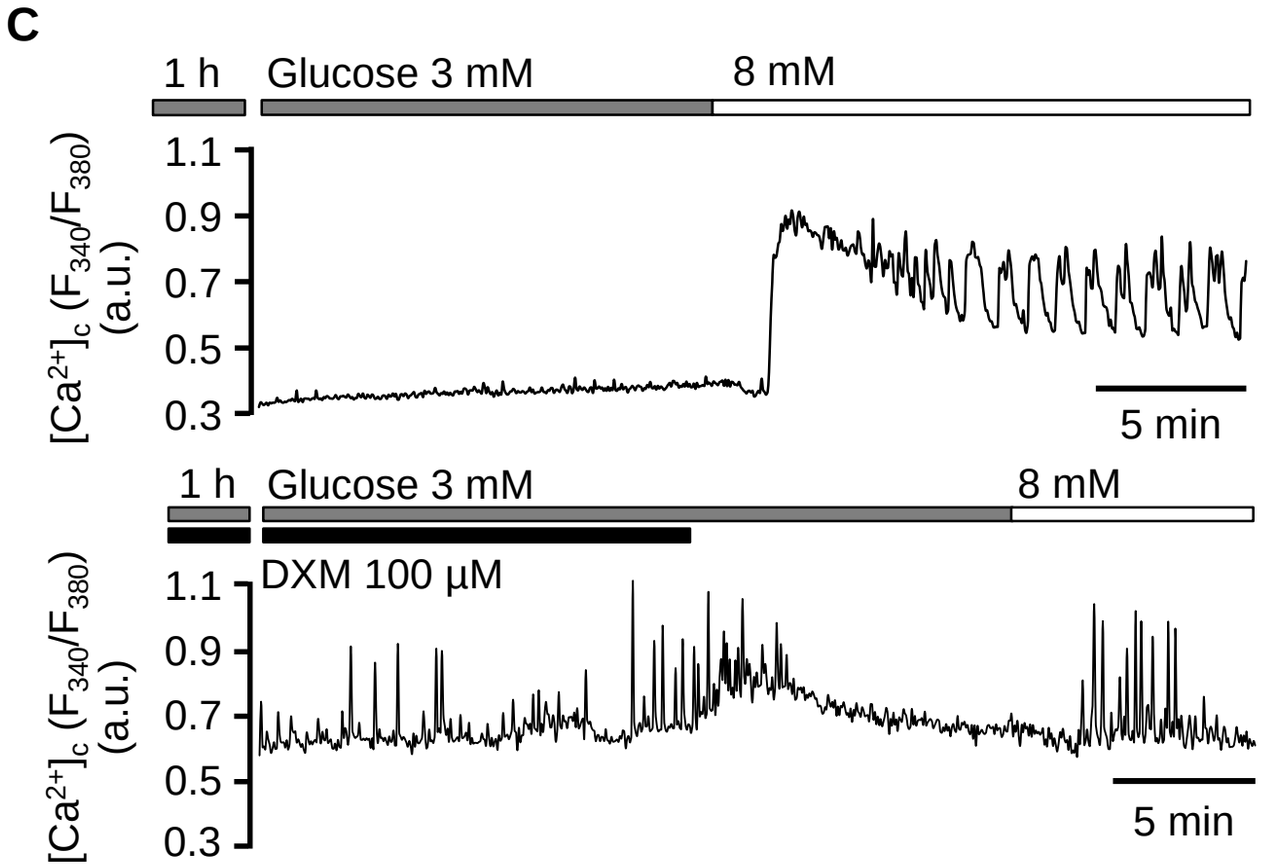

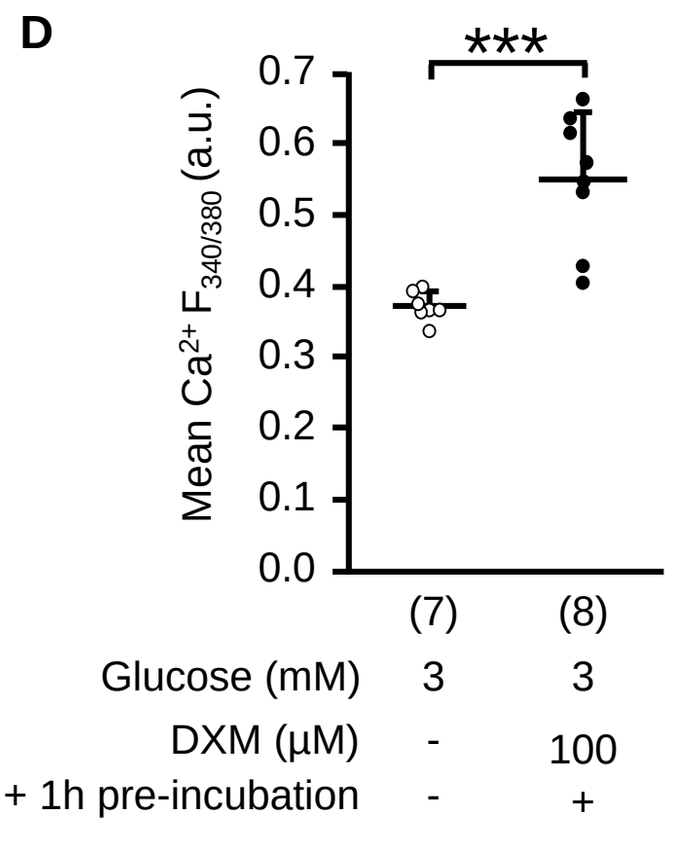

Figure 3

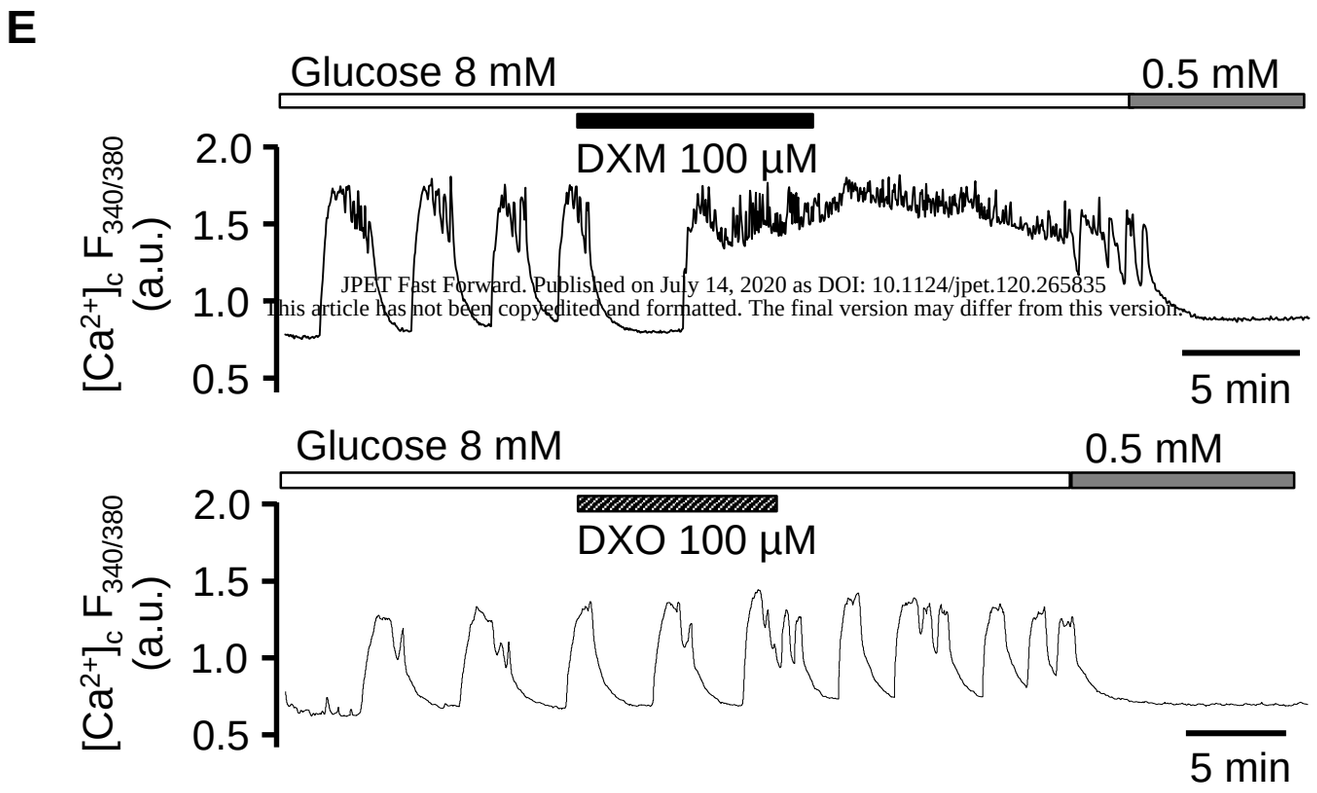

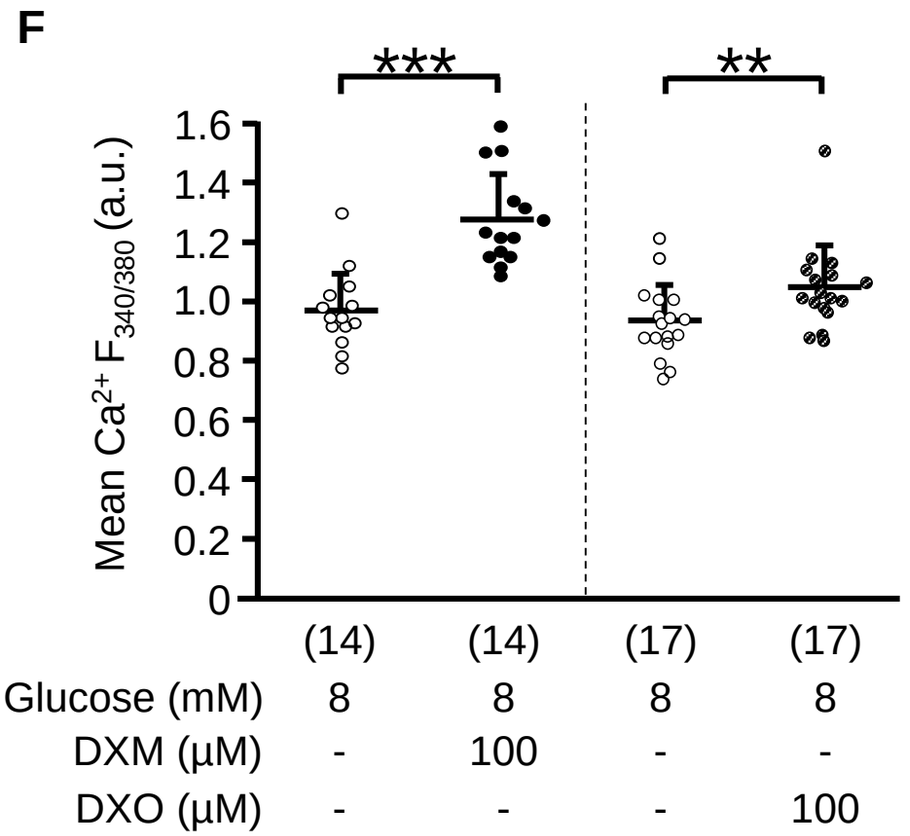

Figure 4

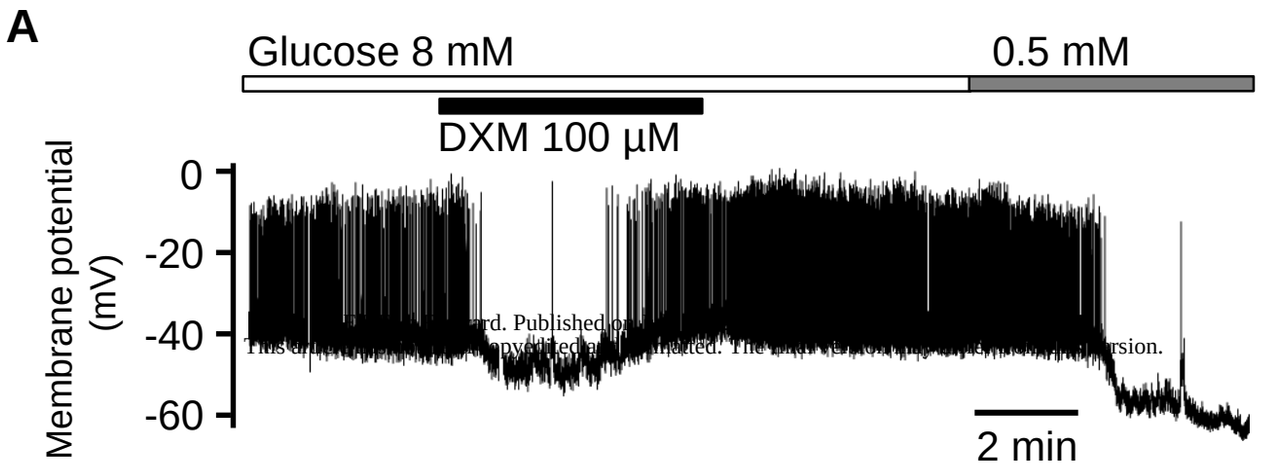

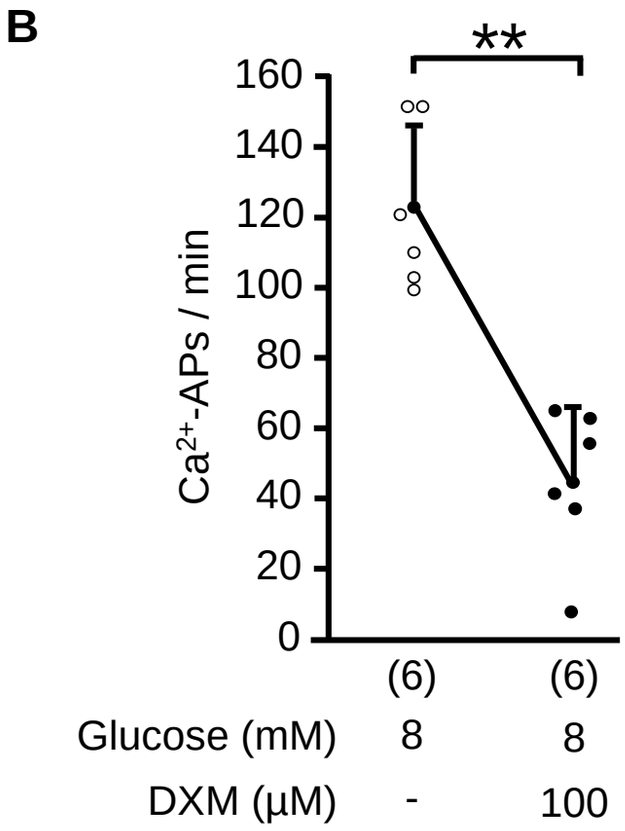

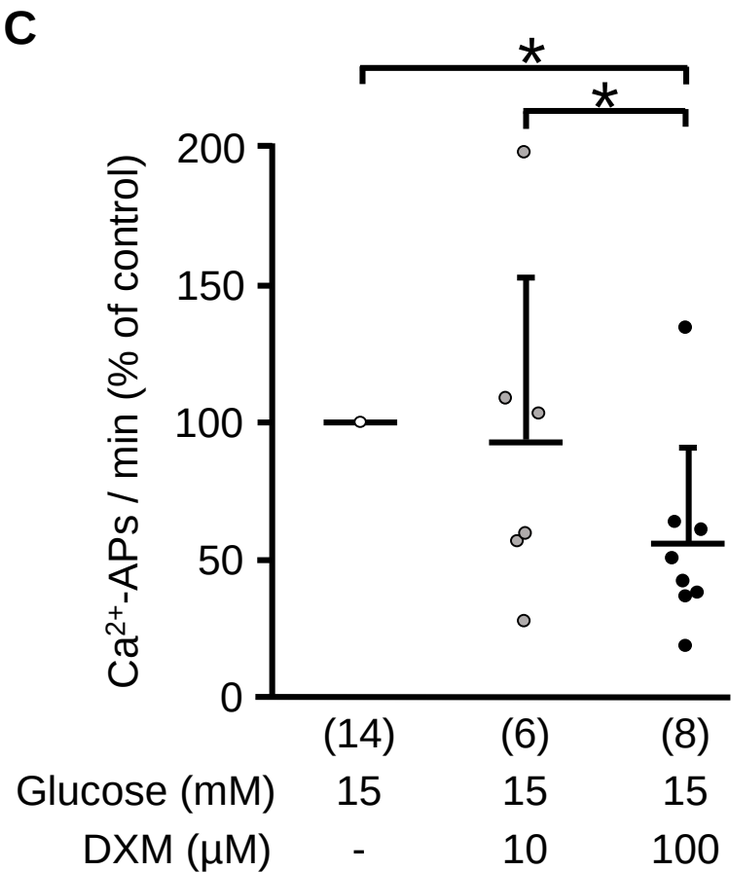

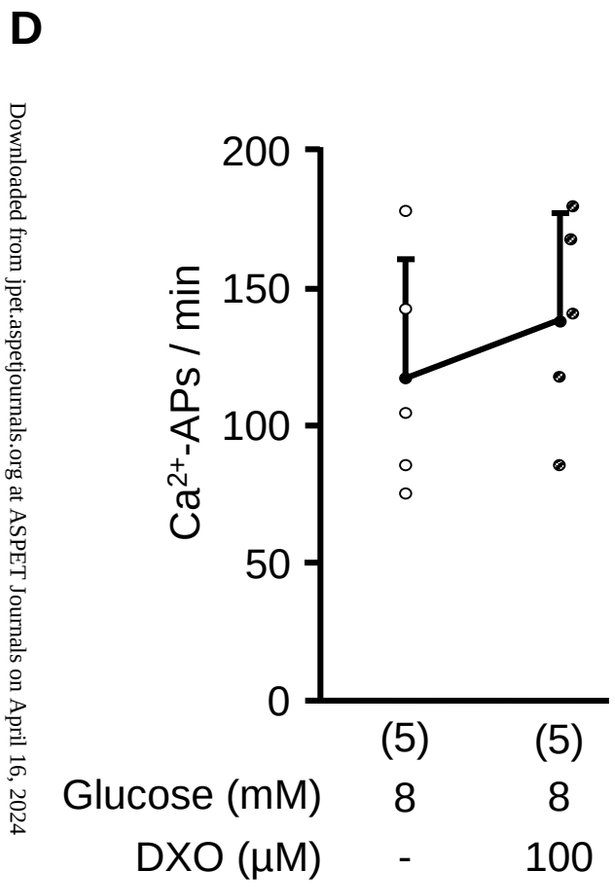

Figure 5

Figure 6